High frequency behaviours and Mössbauer study of field annealed FeCuNbSiB alloy ribbons*

Ma Xiao-Ming(马小明), Li Zhi-Wei(李志伟), Wei Jian-Qiang(位建强), Wang Tao(王 涛)†, and Li Fa-Shen(李发伸)

Institute of Applied Magnetics, Key Laboratory for Magnetism and Magnetic Materials of the Ministry of Education, Lanzhou University, Lanzhou 730000, China

(Received 31 January 2010; revised manuscript received 21 March 2010)

This paper investigates the high frequency behaviours and magnetic anisotropy of rapidly solidified FINEMET ($Fe_{73.5}Si_{13.5}B_9Nb_3Cu_1$) alloy ribbons annealed in an applied magnetic field. It finds that the ribbons annealed with the applied magnetic field show much higher resonance frequencies and have even higher permeability at higher frequencies than the samples annealed without the magnetic field and the non-annealed ribbons. Mössbauer spectroscopy had been employed to study the spatial distribution of the magnetic moments of five selected FINEMET alloy ribbons in different heat-treated conditions. The results show that an easy plane has been established after annealling in the magnetic field, while for the other ribbons this effect is not significant. Hence, the relationship between magnetic field annealing and high frequency property has been bridged by the bianisotropic theory.

Keywords: FINEMET, field annealing, Mössbauer spectrum, high frequency
PACC: 7430G, 3340, 7530

1. Introduction

FINEMET type nanocrystalline alloys have been widely investigated due to their tremendous potential for applications[1,2] and their fundamental theoretical interests[3,4] immediately after the discovery of $Fe_{73.5}Si_{13.5}B_9Nb_3Cu_1$.[5] Previous studies have shown that the appropriate heat treatment of this family of alloys can produce the homogeneous ultrafine grain structure of α-FeSi embedded in the amorphous matrix with a typical grain diameter of 10 nm.[4,6] This will cause a drastic reduction in the magnitude of saturation magnetostriction and the intrinsic coercivity due to the exchange-coupling interaction of the nanograins, and thus leads to a considerable improvement of the soft magnetic properties. Many studies, including the effect of both the substitution of various elements[7−10] and heat treatment conditions,[9−12] have been conducted to develop FINEMET type alloys with remarkable soft magnetic properties. However, most of the studies have focused on the structural and low frequency magnetic properties.[2,3,13,14] To the best of our knowledge, only limited contributions have been done to investigate their properties in high frequency ranges[15,16] in the form of flake-shaped FINEMET alloy particles. The results of their experiments show very promising properties for high frequency applications. Therefore, it is significant to explore the high frequency properties of the FINEMET alloy ribbons since high permeability at high frequencies of the magnetic materials is a persistent requirement for the ceaseless increase of the working frequency.[17−19]

According to the famous formula:[20]

$$(\mu_{\rm i} - 1) f_{\rm r} = \frac{4}{3}\gamma M_{\rm s}, \tag{1}$$

where $f_{\rm r}$ is the the resonance frequency, $\mu_{\rm i}$ is the initial permeability, $M_{\rm s}$ is the saturation magnetization and γ is the gyromagnetic ratio. The product of the $f_{\rm r}$ and $(\mu_{\rm i}-1)$ can not exceed a constant which is known as Snoek limit and only decided by the $M_{\rm s}$. However, it was reported recently in Ref. [21] that the Snoek limit of the material with the bianisotropic model can be regulated by the two anisotropic fields: out-plane anisotropic field ($H_{\rm ha}$) and in-plane anisotropy field ($H_{\rm ea}$), which are effective anisotropy fields when the magnetization deviates from the easy axis in the hard plane and in the easy plane, respectively. The presence of an easy magnetization plane in magnetic materials is the basic condition for the bianisotropic model.

*Project supported by National Natural Science Foundation of China (Grant No. 10774061).
†Corresponding author. E-mail: wtao@lzu.edu.cn
© 2010 Chinese Physical Society and IOP Publishing Ltd

The detailed formation of the formula is[21]

$$(\mu_{\rm i}-1)f_{\rm r}=\frac{\gamma}{2\pi}\sqrt{\frac{H_{\rm ha}}{H_{\rm ea}}}M_{\rm s}. \quad (2)$$

In this paper, in order to induce an easy magnetization plane, the FINEMET alloy ribbon was annealed in an external magnetic field, then the high frequency properties were also investigated. As expected, the ribbons annealed with an applied magnetic field indeed show much higher resonance frequency and have even higher permeability at the high frequency range than the samples annealed without the magnetic field and the non-annealed ribbons.

Additionally, in order to probe the origin of this improvement in the atomic scale, Mössbauer spectroscopy was employed to study the spatial distribution of the magnetic moments of the FINEMET alloy ribbons. It is well established that the relationship between the angle θ and the relative intensities of the ^{57}Fe Mössbauer lines is given by[22]

$$I_{1,6}:I_{2,5}:I_{3,4}=3(1+\cos^2\theta):4\sin^2\theta:(1+\cos^2\theta), \quad (3)$$

where θ is the angle between the magnetic moment and the γ ray. The calculated θ value should be 55° for spatially isotropic distribution of the magnetic moments.

2. Experimental details

The as-quenched amorphous ribbons with the nominal composition of $Fe_{73.5}Si_{13.5}B_9Nb_3Cu_1$ were prepared by melt spinning technique which were supplied by ShenZhou Electronic Technology Company of Lin Yi. The width and thickness of the ribbons are 35 mm and 20 μm, respectively. These ribbons were heat-treated under different conditions and five of the samples were selected in this paper, namely, the as-quenched sample, sample A, sample B, sample C and sample D, and the detailed annealing conditions are listed in Table 1. The applied magnetic field was 2500 Oe (1 Oe=79.5775 A/m) and the ribbons were annealed for an hour and cut into appropriate shapes for measurements

The structural changes were characterized by a x-ray diffractometer (XRD) (Philips X'Pert) with Cu Kα radiation. The static magnetic properties were recorded on a vibrating sample magnetometer (VSM, Lake Shore 7304) and the saturation magnetization of samples are listed in Table 1. The values of complex permeability of the samples were obtained by an Agilent E8363B Vector Network Analyser with a microstrip method[23] in the 0.1–5 GHz range. The direction of microwave magnetic field was in the plane of the ribbon and perpendicular to the direction of the applied magnetic field during annealing for field-annealed samples. Mössbauer measurements were performed at room temperature using conventional constant acceleration type spectrometer in transmission geometry. The gamma-ray source is 25 mCi^{57}Co in Palladium matrix and the driver velocity was calibrated using an α-Fe foil. All the spectra were fitted with the hyperfine field distribution by a slightly modified version of the Hesse and Rübartsch method using the MossWinn programme.[24,25]

Table 1. Annealing conditions and values of saturation magnetization of samples under investigation.

ID	annealing temperature /°C	annealing time /h	applied magnetic field /Oe	$M_{\rm s}$ /(emu/g)
as-quenched	—	—	—	146.28
A	450	1	0	150.25
B	450	1	2500	154.37
C	540	1	0	141.42
D	540	1	2500	154.72

3. Experiment results and discussion

Figure 1 shows XRD patterns of the $Fe_{73.5}Si_{13.5}B_9Nb_3Cu_1$ ribbons before and after heat treatment. The as-quenched ribbon and the two samples annealed at 450 °C all show a broad diffraction peak, which is due to the amorphous structure. It can be confirmed that the crystalline phase can not appear in the ribbons annealed at 450 °C, which is consistent with previous reports.[26,27] For the 540 °C heat-treated ribbons, higher and sharper

diffraction lines are observed. The diffraction peaks could be indexed as the Fe_3Si nanocrystalline phase with DO_3 structure. According to the Sherrer formula, the average crystalline size of the nano-grains is about 12 nm for both the non-field and field annealed samples, which is in good agreement with previous reported results.[13,28] However, the XRD results do not give significant differences between the field annealed and non-field annealed samples treated at the same temperature. Moreover, the values of the saturation magnetization of all samples which are listed in Table 1 show no obvious change.

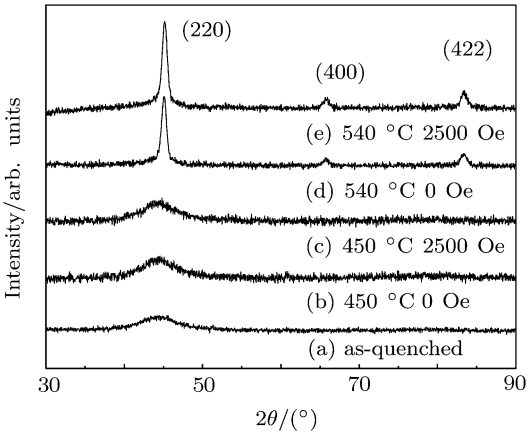


Fig. 1. The XRD patterns for samples: (a) as-quenched sample; (b) sample A; (c) sample B; (d) sample C; (e) sample D.

3.1. Sample A and sample B

Figure 2 shows the the complex permeability, (a) real part and (b) imaginary part, as a function of frequency for as-quenched ribbon, sample A and sample B. For the as-quenched sample and sample A, the imaginary part values do not show absorption peak in the 0.1–5 GHz range.

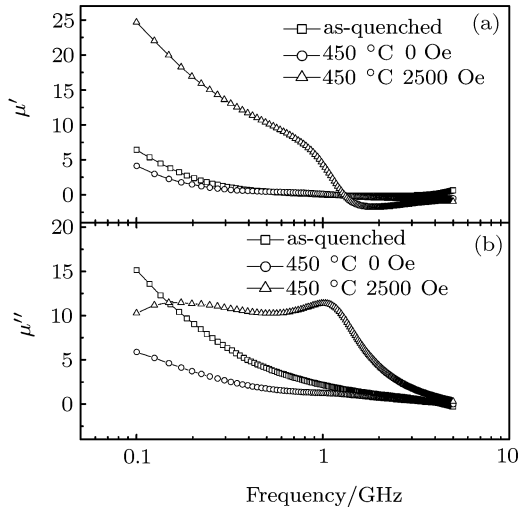


Fig. 2. The real part (a) and the imaginary part (b) of the complex permeability of the $Fe_{73.5}Si_{13.5}B_9Nb_3Cu_1$ ribbons in indicated annealing conditions.

However, for sample B the imaginary part of the spectrum shows obvious absorption peak at 1.0 GHz. With the nearly same value of saturation magnetization, the high frequency properties of the sample A and sample B are quite different. For sample A annealed at 450 °C without the magnetic field, the results show no obvious changes in comparison with the as-quenched sample, but the resonance frequency of sample B reaches 1.0 GHz, and the permeability maintains a relative high value in the measurement frequency range.

In order to investigate the changes of the magnetization state in the atomic scale, Mössbauer spectroscopy was performed to study the samples at different annealing conditions. The Mössbauer spectra shown in Fig. 3 of as-quenched ribbon, sample A and sample B all exhibit an asymmetrical sextet with broad and overlapped lines, which is typical for amorphous alloys. A linear relationship between the magnetic hyperfine field and the isomer shift was introduced to reproduce the asymmetrical shape of the spectra and the hyperfine parameters are in Table 2. Comparing the spectrum of sample B with that of sample A, obviously we find that the intensity of 2,5 peaks has been enhanced and according to the formula (3), and list the calculated values of the mean angle θ of the samples in Table 2. The angle θ of the as-quenched ribbon is 59° which is a little bigger than 55°. This may be explained as that, due to the magnetostriction caused by rapid solidification,[29] a small number of the magnetic moments are confined to parallel the ribbon plane. With proper heat treatment, the magnetostriction will be released and hence leads to a spatially isotropic distribution of the magnetic moments, which can be confirmed by the value of the angle, 56°, of sample A. It should be noted that though the thickness of the ribbon is only 20 μm, the demagnetization effect is still unable to propel the magnetic moments in the ribbon plane. However, the magnetic moments of sample B are inclined to lie in the plane of the ribbon and the angle is 72° for sample B due to the effect of field annealing.

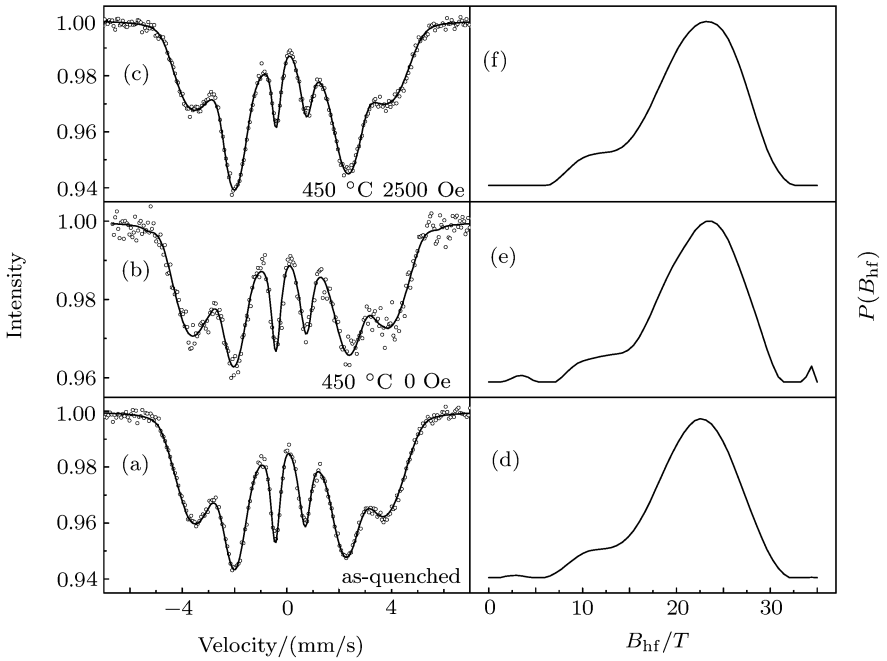


Fig. 3. The Mössbauer spectra obtained from: (a) as-quenched sample; (b) sample A; (c) sample B. The corresponding distribution of hyperfine field is given on the right.

Table 2. Hyperfine parameters for samples under investigation.

sample	δ/(mm/s)	Γ/(mm/s)	B_{hf}/T	$(I_{2,5}/I_{3,4})$/arb. units	θ/(°)
as-quenched	0.10	0.36	21.22	2.31	58.8
A	0.13	0.39	22.74	2.07	55.7
B	0.13	0.37	21.50	3.30	72.0
C	0.24	0.27	22.81	2.59	62.4
D	0.14	0.27	22.46	3.94	85.0

It should combine the results of permeability and the values of angles to analyse the high frequency property of sample B. As is well known, an easy magnetization direction can be induced to parallel the direction of the magnetic field applied during annealing for the magnetic materials.[30,31] In our case, an easy magnetization plane is well established for the field-annealed ribbon. Base on the above analysis, we may assume that the out-plane anisotropic field (H_{ha}) for the field annealing ribbon is much larger than the in-plane anisotropic field (H_{ea}). In this situation the Snoek limit is obviously reconciled by the two anisotropy field. According to Eq. (2), it is not difficult to understand that the initial permeability and the resonance frequency are improved simultaneously.

In order to illustrate that the presence of the easy magnetization plane can result in improvement of high frequency properties of the FINEMET alloy ribbons further, two ribbons annealed at 540 °C with and without an external field respectively were also investigated.

3.2. Sample C and sample D

The measured frequency dependence of real and imaginary part of permeability for samples C and D is shown in Figs. 4(a) and 4(b). As can be seen, both the real and imaginary parts of the complex permeability of sample C are enhanced in comparison with the as-quenched sample, and the resonance frequency is 0.22 GHz. For sample D the real part of the permeability is increased to 40 at 0.1 GHz, and the resonance frequency has been enhanced to 0.43 GHz. The Mössbauer spectra of samples C and D, which are shown in Fig. 5, exhibit a complex hyperfine structure in which the sharp lines corresponding to the nanocrystalline grains are superimposed with the broad overlapped lines attributed the residual amorphous matrix. Hyperfine parameters of the ribbons extracted by fitting the spectra are listed in

Table 2. The fitted spectra and the hyperfine field distribution clearly show the transition from amorphous to nanocrystalline state by annealing at 540 °C.

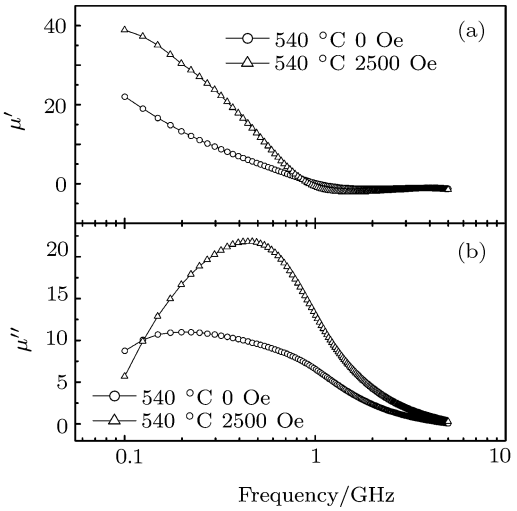


Fig. 4. The real part (a) and the imaginary part (b) of the complex permeability of the $Fe_{73.5}Si_{13.5}B_9Nb_3Cu_1$ ribbons in indicated annealing conditions.

The hyperfine magnetic field and the isomer shift of the two heat treated ribbons are very similar and are in good agreement with reported results.[29,32] However, as shown in Table 1 the spatial distributions of the magnetic moments of the two samples are different, the value of the mean angle between the magnetic moments and the γ ray is 62° for sample C but 85° for sample D.

For sample C, the mean angle is a little larger than that of sample A and the high frequency magnetic properties of these two samples also show obvious differences. It should combine the results of XRD with Mössbauer spectra to understand this phenomenon. From the XRD results, it can be obtained that sample A is still in the amorphous state, so the distribution of the magnetic moments is randomly distributed, but sample C contains many α-FeSi nanograins. The presence of the crystalline phase makes the magnetic dipole effect dominate the spin–orbit interaction, which makes the magnetic moments orientation prone to parallel the plane of the ribbon.[33] As some magnetic moments lie in the plane of the ribbon, the out-plane anisotropy has been formed. The Snoek limit is varied due to the weak anisotropy, so the high frequency magnetic properties have been improved.

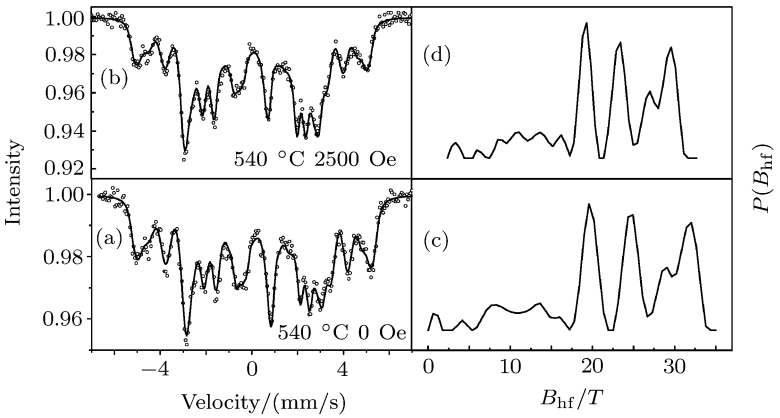


Fig. 5. The Mössbauer spectra obtained from: (a) sample C; (b) sample D. The corresponding distribution of hyperfine field is given on the right.

For sample D, it has been found that the mean angle is close to 90° again, which illustrates that most magnetic moments are lying in the plane of the ribbon. It means that a nearly perfect easy magnetization plane, the basic condition to form the bianisotropic model, has been formed. Just as the previous analysis of sample B, an easy magnetization direction can be induced in the plane of the ribbon.[30,31] Therefore, the permeability and resonance frequency increase simultaneously as the Snoek limit has been modified by the two anisotropic fields.

4. Conclusion

In summery, two series of $Fe_{73.5}Si_{13.5}B_9Nb_3Cu_1$ alloy ribbons annealed at different conditions were investigated in this paper. It was found that the ribbons annealed with the applied magnetic field show much

higher resonance frequency and have much higher permeability at higher frequency range than the as-quenched and non-field annealing samples. Mössbauer results show that the high frequency is strongly effected by the distribution of magnetic moments at the micro scale and the establishment of an easy magnetization plane plays an important role in improving the high frequency behaviours. The results can be well explained by the bianisotropic theory, and the heat-treated $Fe_{73.5}Si_{13.5}B_9Nb_3Cu_1$ ribbons show promising potential for high frequency applications.

References

[1] Petzold J 2003 *Scripta Mater.* **48** 895

[2] Kim G H, Noh T H, Choi G B and Kim K Y 2003 *J. Appl. Phys.* **93** 7211

[3] Gorria P, Garitaonandia J S and Barandiarán 1996 *J. Phys.: Condens. Mat.* **8** 5925

[4] Prabhu D, Narayanasamy A, Ganesan K, Ponpandian N and Chattopadhyay K 2007 *J. Alloys Compd.* **438** 15

[5] Yoshizawa Y, Oguma S and Yamauchi K 1988 *J. Appl. Phys.* **64** 6044

[6] Shahri F, Beitollahi A, Shabestari S G, Ghanaatshoar M, Tehranchi M M, Mohseni S M, Roozmeh S E, Wanderka N and Fiorillo F 2007 *J. Magn. Magn. Mater.* **312** 35

[7] Franco V, Conde C F, Conde A and Ochin P 2001 *J. Non-Cryst. Solids* **287** 366

[8] Borrego J M, Conde C F and Conde A 2001 *Mater. Sci. Eng.* **304–306** 491

[9] Frost M, Todd I, Davies H A, Gibbs M R J and Major R V 1999 *J. Magn. Magn. Mater.* **203** 85

[10] Szumiata T, Górka B, Zorkovská A and Sovák P 2005 *J. Magn. Magn. Mater.* **295** 95

[11] Varga L K, Mazaleryrat F, Kovács Gy and Kákay A 2001 *J. Magn. Magn. Mater.* **226–230** 1550

[12] Blázquez J S, Franco V, Conde C F and Conde A 2003 *J. Magn. Magn. Mater.* **254–255** 460

[13] Fernández Barquín L, Gómez J C, Gorria P, Garitaonandia J S and Barandiarán 1998 *J. Phys.: Condens. Mat.* **10** 5027

[14] Kolano-Burian A, Varga L K, Kolano R, Kulik T and Szynowski J 2007 *J. Magn. Magn. Mater.* **316** e820

[15] Qiao L, Wen F S, Wei J Q, Wang J B and Li F S 2008 *J. Appl. Phys.* **103** 063903

[16] Yang W F, Qiao L, Wei J Q, Zhang Z Q, Wang T and Li F S 2010 *J. Appl. Phys.* **107** 033913

[17] Rozanov K N, Li Z W, Chen L F and Koledintseva 2005 *J. Appl. Phys.* **97** 013905

[18] Matsushita N, Nakamura T and Abe M 2003 *J. Appl. Phys.* **93** 7133

[19] Seemann K, Leiste H and Bekker V 2004 *J. Magn. Magn. Mater.* **283** 310

[20] Snoek J L 1948 *Physica* **14** 207

[21] Xue D S, Li F S, Fan X L and Wen F S 2008 *Chin. Phys. Lett.* **25** 4120

[22] Zhou D, Li Z W, Yang X, Wen F S and Li F S 2008 *Chin. Phys. Lett.* **25** 1865

[23] Bekker V, Seemann K and Leiste H 2004 *J. Magn. Magn. Mater.* **270** 327

[24] Hesse J and Rübartsch A 1974 *J. Phys.* E *Sci. Instr.* **7** 526

[25] Klencsár Z, Kuzmann E and Vértes A 1996 *J. Radioanal. Nucl. Chem.* **210** 105

[26] Hampel G, Pundt A and Hesse J 1992 *J. Phys.: Condens. Mat.* **4** 3195

[27] Shahri F, Beitollahi A, Shabestari S G and Kamali S 2007 *Phys. Rev.* B **76** 024434

[28] Huong P M, Peng H X, Wisnom M R, Yu S C and Chau N 2006 *Composites:* Part A **37** 191

[29] Knobel M and Sato T R 1992 *J. Appl. Phys.* **71** 6008

[30] Miguel C, Zhukov A P and Gonzalez J 2001 *J. Non-Cryst. Solids* **287** 355

[31] Benda O, Bydžovský and Herzer G 1995 *J. Magn. Magn. Mater.* **140–144** 479

[32] Rixecker G, Schaaf P and Gonser U 1992 *J. Phys.: Condens. Mat.* **4** 10295

[33] Li X D, Yuan W Z, Zhao Z J, Wang X Z, Ruan J Z and Yang X L 2004 *J. Magn. Magn. Mater.* **279** 429